

SUPPLEMENTAL MATERIAL

The COMMD Family Regulates Plasma LDL Levels and Attenuates Atherosclerosis Through Stabilizing the CCC complex in Endosomal LDLR Trafficking

Alina Fedoseienko^{1,11}, Melinde Wijers^{1,11}, Justina C. Wolters¹, Daphne Dekker¹, Marieke Smit¹, Nicolette Huijkman¹, Niels Kloosterhuis¹, Helene Klug², Aloys Schepers³, Ko Willems van Dijk⁴, Johannes H. M. Levels⁵, Daniel D. Billadeau⁶, Marten H. Hofker^{1,12}, Jan van Deursen^{7,8}, Marit Westerterp¹, Ezra Burstein⁹, Jan Albert Kuivenhoven¹, Bart van de Sluis^{1,10}

Department of Pediatrics, Molecular Genetics Section, University of Groningen, University Medical Center Groningen, Groningen, The Netherlands¹; PolyQuant GmbH, Bad Abbach, Germany²; Monoclonal Antibody Core Facility and Research Group, Institute for Diabetes and Obesity, Helmholtz Zentrum, München³; Department of Human Genetics and Department of Medicine, division Endocrinology, Leiden University Medical Center, Leiden, The Netherlands⁴; Department of Vascular and Experimental Vascular Medicine, Academic Medical Center, University of Amsterdam, Amsterdam, The Netherlands⁵; Department of Immunology and Biochemistry, Division of Oncology Research, Mayo Clinic, Rochester, USA⁶; Department of Pediatrics and Adolescent Medicine⁷ and the Department of Biochemistry and Molecular Biology⁸, Mayo Clinic College of Medicine, Mayo Clinic, Rochester, Minnesota, USA; University of Texas Southwestern Medical Center, Dallas, TX, USA⁹; University of Groningen, University Medical Center Groningen, iPSC/CRISPR center Groningen, The Netherlands¹⁰.

¹¹These authors contributed equally to this work

¹²Marten H. Hofker deceased during preparation of this manuscript

Corresponding author: a.j.a.van.de.sluis@umcg.nl

Methods

Animals

Commd6 conditional knockout mice were generated using the multi-purpose targeting vector pNTKV1901-frt/loxP.¹ Cloning of the targeting construct was performed as previously described.¹ Using homologous recombination in embryonic stem (ES) cells, we introduced a neomycin (neo) cassette with a cryptic acceptor and donor site in intron 3, and *loxP* sites flanking exon 3 (Fig. 1A). The neo cassette was flanked with frt sites (Fig. 1A). The *NotI*-linearized targeting vector was electroporated into TL1 129Sv/E ES cells. After selection with G418 and expansion, the presence of the conditional *Commd6* allele was confirmed by Southern blot analysis (Fig. 1A). We produced chimeric mice by microinjecting two independent ES cell-targeted clones into C57BL/6 blastocysts. Next, we crossed chimeric males with C57BL/6 females and the mutated *Commd6* allele was successfully transmitted to their offspring. We crossed the mutated *Commd6* mice with ROSA26::FLPe mice (The Jackson Laboratory stock#009086) to excise the neo gene cassette. Then, mice were backcrossed to a C57BL/6 genetic background for at least six generations, before crossing with Alb-Cre mice (The Jackson Laboratory stock#003574) to generate liver-specific *Commd6* knockout mice. The following primers were used to genotype the mice: floxed *Commd6* forward (5'-AGGGCTTGAGTATGGGACAG-3') and reverse (3'-GTGAGAAATACCACTGCCTTG-5'); *Alb-Cre* forward (5'-GCGGTCTGGCAGTAAAACTATC-3') and reverse (5'-ACGAACCTGGTCGAAATCAGTG-3'). *Commd6* conditional knockout mice have been submitted to The Jackson Laboratory (stock#031057).

Liver-specific *Commd1* knockout mice were previously described.² *Commd9* ablation in hepatocytes was accomplished by crossing floxed *Commd9* mice³ with Alb-Cre mice (#003574, The Jackson Laboratory). Rosa26-LSL-Cas9 knock in mice (#024857, The Jackson Laboratory)⁴ were crossed with Alb-Cre mice to generate liver-specific Cas9-expressing mice, and were used to target *Ccdc22* in mouse livers through CRISPR/Cas9 gene editing technology.

Except for the atherosclerosis study, in any other studies we used male mice. Mice were housed individually and fed *ad libitum* with either a standard rodent chow diet (RMH-B, AB Diets, the Netherlands) or, starting at 10 weeks of age, a high-fat, high-cholesterol (HFC) diet (45% calories from butter fat, containing 0.2% cholesterol, SAFE Diets), n=5–9. Mice were fed a HFC diet for 1 week, and mice were fasted for 4 hours before the mice were sacrificed. In all experiments littermates, which are homozygous floxed mice without the Cre-allele, were used as wild type (WT) controls.

To generate a hepatic LDLR-deficient background, *Commd1*^{ΔHep} mice and WT littermates were injected via the orbital vein with 3.0×10^{11} vector genomes of AAV-PCSK9-D377Y⁵ (n=9-10). Volumes of injection were adjusted to 100 μ l with sterile phosphate-buffered saline (PBS).

For atherosclerosis measurements, ten weeks old female ApoE3*Leiden;*Commd1*^{F/F}; Alb-cre (ApoE3*L;*Commd1*^{ΔHep}) and ApoE3*Leiden;*Commd1*^{F/F} (ApoE3*L) mice were fed a HFC diet for 12 weeks (n=9-12). After 12 weeks of HFC diet, mice were sacrificed, blood was collected and the heart was fixed by cold isopentane for histology. Cross-sections of 6 μ m were made throughout the aortic root area of the heart and sections were stained with Toluidin blue. Slides were scanned with a Hamamatsu slide scanner. The average lesion size was determined from ten sections for each animal with a 24 μ m interval. Plaque size was measured in a blinded fashion using image scope software (Leica Aperio Imagescope). The aortic arch was dissected, fixed in formalin and stained for lipid deposits using Oil Red-O, and pinned on silicon-coated dishes. Oil Red O positive areas were quantified using Image J.

Tissues for mRNA and protein expression analysis were snap-frozen in liquid nitrogen and stored at -80°C until further analysis. Blood was drawn by cardiac puncture, and plasma was collected after centrifugation at 3000 rpm for 10 min at 4°C. All animal studies were approved by the Institutional Animal Care and Use Committee, University of Groningen (Groningen, the Netherlands).

Fast-performance liquid chromatography (FPLC) of single plasma samples

Cholesterol concentrations in the main lipoprotein classes (VLDL, LDL and HDL) were determined using fast protein liquid chromatography (FPLC) as described previously with some minor modifications.⁶ The system contained a PU-980 ternary pump with an LG-980-02 linear degasser, FP-920 fluorescence and UV-975 UV/VIS detectors (Jasco, Tokyo, Japan). An extra PU-2080i Plus pump (Jasco, Tokyo, Japan) was used for in-line cholesterol PAP or Triglyceride enzymatic reagent (Roche, Basel, Switzerland) addition at a flowrate of 0.1 ml/min. Plasma lipoproteins were separated with a

Superose 6 HR 10/30 column (GE Healthcare Hoevelaken, The Netherlands) using TBS pH 7.4, as eluent at a flow rate of 0.31 ml/min. Quantitative analysis of the chromatograms was carried out with ChromNav chromatographic software, version 1.0 (Jasco, Tokyo, Japan). Commercially available lipid plasma standards (low, medium and high) were used for quantitative analysis (SKZL, Nijmegen, the Netherlands) of the separated lipoprotein fractions.

RNA interference

COMMD1 was stably silenced in HEK293T and HepG2 cells using shRNA as previously described.⁷ A plasmid encoding short hairpin RNA against COMMD6 was generated by cloning a target sequence specific for human COMMD6 (AATGACGATTCCACAGTTTCA) or mouse COMMD6 (TGACAATTCCACAATTTCA) into the pLKO-TRC vector. HEK293T, HepG2 and RAW264.7 cell lines were infected with lentiviral particles carrying the pLKO-TRC or pLKO-shCOMMD6 vector. To produce lentiviral particles, HEK293T cells were transfected with pLKO-TRC or pLKO-shCOMMD6 together with pMDLg-pRRE, pH-CMV-G and pRSV-Rev packaging plasmids using FuGENE-6 transfection reagent (Promega) at a Fugene to DNA ratio of 3:1. Virus-containing supernatant culture medium was filtered (0.45 micron, Corning), mixed with polybrene (4 mg/ml) and used for infection for three consecutive 12 hour periods. Twenty-four hours after the third infection, the culture medium was supplemented with puromycin (1 µg/ml).

Sucrose Gradients

Male mice (WT and *Commd1*^{ΔHep}) were fasted for 4 h and sacrificed. Livers were isolated, and processed as described previously.

In short, 200 mg of liver was homogenized in 800 µl homogenization buffer (50 mM Tris-HCl, pH 7.4, 250 mM sucrose, 25 mM KCl, 5 mM MgCl₂, 3 mM imidazole, Roche protease inhibitor mixture) with 20 strokes in a Dounce homogenizer. Homogenates were centrifuged (1000xg, 10 min at 4°C) to remove nuclei and other debris. A unit of 300 µg of liver homogenates was loaded on a 3.7-ml continuous 10-40% sucrose gradient and centrifuged using a Beckman Coulter SW55 Ti rotor for 16 h at 40,000 rpm. 285 µl fractions were collected from the bottom by puncture the bottom of the tube with a 20-gauge needle. 1/10 of each fraction were mixed SDS sample buffer and used for Western blot analyses.

Immunoprecipitation analysis

Immunoprecipitation experiments were performed as described before.⁷ Cells were lysed in NP-40 buffer (0.4M NaCl, 0.1% NP-40, 10mM Tris-HCl, pH 8.0 and 1mM EDTA), supplemented with protease inhibitors. In this study HEK293T cells and primary hepatocytes were used. Mouse anti-COMMD1 (MAB7526, R&D Systems) antibodies were used to immunoprecipitate COMMD1, rabbit anti-COMMD6 (custom made⁸) was used to immunoprecipitate COMMD6. Normal IgG was used as a negative IP control.

Immunofluorescence

HEK293T cells were cultured for 24 h on coverslips, fixed in ice-cold fixative (4% paraformaldehyde and 0.5% glutaraldehyde in PBS) and incubated for 18 min in the dark at room temperature, followed by permeabilization for 4 min with 0.2% Triton X-100 in PBS. Cells were subsequently incubated with primary antibodies at 4°C in a humidified chamber. Following three washes in PBS, cells were incubated with secondary antibodies (1:500 dilution in blocking buffer) for 1 h at room temperature or overnight at 4°C in a humidified chamber. After three washes in PBS, coverslips were mounted on slides with Vectashield mounting medium containing DAPI (Vector Laboratories; H-1200). Images were obtained with a Zeiss Axio Imager2 with Apotome 2 with a Plan-APOCHROMAT 63x/1.4 oil objective, using ZEN software (Zeiss).

Adenovirus generation for somatic gene editing by CRISPR/Cas9 technology

Three guide RNAs, targeting either exon 1 or exon 2 of murine *Ccdc22* (Fig. 6A), were separately cloned into a *BbsI*-digested pSpCas9(BB)-2A-Puro (PX459) plasmid (Addgene plasmid# 48139) to create U6-guideRNA-sgRNA scaffold cassettes. These cassettes were amplified by PCR using the following primers: forward sg#1: 5'-GTCGACgagggcctatttccatgat-3'; reverse sg#1: 5'-GGATCCAAAAAagcaccgactcgtg -3'; forward sg#2: 5'- GGATCCgagggcctatttccatgat-3'; reverse

sg#2: 5'-tctagaAAAAAAGcaccgactcggtg-3'; forward ##: 5'-TCTAGAAGagggcctatttccatgat-3'; reverse sg#3: 5'-gcggccgcAAAAAAGcaccgactcggtg-3', and were ligated into a *SaII-NotI*-linearized pENTR2B entry plasmid (Invitrogen #11816-014). The construct sequence is available upon request. A LR recombination reaction (Invitrogen #11791-020, following manufacturer's protocol) with pAd/pL-Dest was performed to obtain the adeno-expression construct. For virus production, 4 ug of *PacI*-digested expression vector was transfection into HEK293A cells (Invitrogen # R705-07). Visible virus production was observed after 9 days. Reproduction and upscaling of the virus was performed in five steps, and produced up to 7500 cm² infected HEK293A cells. Viruses were purified using cesium chloride density gradients, and stored at -80°C at a concentration of 7.45x10¹² particles per ml.

AV particles were injected intravenously in 9–10 week old mice expressing Cas9 specifically in the liver (see material and method section: animals). All AV doses were 1x10¹¹ particles and adjusted to 100 µl with sterile phosphate-buffered saline (PBS). Blood was collected by retro-orbital bleeding one week before virus administration, and mice were sacrificed 3 weeks after administration.

COMMD6-V5 tag fusions by CRISPR/Cas9 gene editing technology

To fuse a V5-tag to endogenous *COMMD6* of HEK293T cells we used CRISPR/Cas9 gene editing technology. The homology construct for specific integration of the V5-tag was assembled in pBluescriptII KS+ vectors. The left (225 bp) and right (280 bp) homology arms and the V5-tag flanking the stop codon were cloned into the vector using standard cloning techniques. Primer sequences are available upon request. gRNAs were designed using the online MIT CRISPR designer tool, and cloned into the pX459 vector (Addgene plasmid #48139). The guide sequence and the homology construct were validated by Sanger sequencing. gRNA efficiency was tested as previously described.⁹ HEK293T cells were transfected with the pX459-sgRNA vector and the V5-tag flanked with the short homology regions (Fig. S2A). Forty-eight hours after transfection, single cells were seeded to form colonies. Two week later, colonies were collected and cultured individually in 96-well plates. Single-cell clones were cultured and correct incorporation of the V5-tag was determined by PCR amplification and sequencing (Fig S2B, C). Western blot analysis with an anti-V5 antibody detected proteins with the expected molecular weight in targeted HEK293T cells but not in control cells (Fig. S2D). In addition, *COMMD6* fused with V5-tag was specifically observed by immunofluorescence in gene edited cells and not in control cells (Fig. S2E).

Gene expression analysis

Cells were grown to 70% confluency and lysed with QIAzol Lysis Reagent (Qiagen). Pieces of murine liver of approximately 100 mg were homogenized in 1 ml QIAzol Lysis Reagent (Qiagen). Total RNA was isolated by chloroform extraction. Isopropanol-precipitated and ethanol-washed RNA pellets were dissolved in RNase/DNase free water. One microgram of RNA was used to prepare cDNA with the Transcriptor Universal cDNA Master kit (Roche), according to the manufacturer's protocol. Twenty nanograms of cDNA was used for subsequent quantitative real-time PCR (qRT-PCR) analysis using the FastStart SYBR Green Master (Roche) and 7900HT Fast Real-Time PCR System (Applied Biosystems). The PCR reaction was performed as follows: 2 min at 50°C, 10 min at 95°C, 40 cycles of 15 sec at 95°C and 1 min at 60°C. Expression data were analyzed using SDS 2.3 software (Applied Biosystems), using the 'standard curve' method of calculation. GAPDH was used as an internal control for human cell lines (HEK293T and HepG2). PPIA expression was used as an internal control for mouse samples and RAW 264.7 cells. Primer sequences are available upon request.

Antibodies

We used the following antibodies: rabbit anti-COMMD1 (11938-1-AP, Proteintech Group, 1:1000), mouse anti-COMMD1 (MAB7526, R&D Systems, 1:100), rabbit anti-COMMD3 (ab176583, Abcam, 1:1000), rabbit anti-COMMD4 (ab115169, Abcam, 1:1000), rabbit anti-COMMD5 (10393-1-AP, Proteintech Group, 1:1000), rabbit anti-COMMD6 (custom made⁸, 1:100), rabbit anti-COMMD9 (192-AP, custom made, Starokadomskyy, 2013, 1:1000), rabbit anti-COMMD10 (GTX121488, GeneTex, 1:1000), rabbit anti-LDLR (PAB8804, Abnova GmbH, 1:1000), rabbit anti-CCDC22 (16636-1-AP, ProteinTech Group, 1:2000), mouse anti-Flag-M2-HRP (A8592, Sigma, 1:2000), HRP-conjugated goat anti-rabbit IgG (H + L) (170-6515, Bio-Rad, 1:10000), HRP-conjugated goat anti-mouse IgG (H + L) (170-6516, Bio-Rad, 1:10000), mouse anti-□-actin (A5441, Sigma-Aldrich, 1:5000); rabbit anti-tubulin

(ab4047, Abcam, 1:2000), rabbit anti-CCDC22 (16636-1-AP, ProteinTech Group, 1:100), rabbit anti-CCDC93 (20861-1-AP, Proteintech, 1:5000), goat anti-VPS35 (ab10099, Abcam, 1:100), mouse anti-V5 (46-0705, Invitrogen, 1:1000), and rabbit anti-V5 (ab9116, Abcam, 1:500). Rabbit polyclonal antibodies against WASH1 (1:1000) and FAM21 (1:100) have previously been described.¹⁰ Anti-apoB100 (1:1000) and rabbit anti-apoA1 (1:1000) antibodies were a gift from Dr. A.K. Groen. For generation of the monoclonal antibody against mouse COMMD6, approximately 50 µg of GST-COMMD6 fusion protein dissolved in PBS was emulsified in an equal volume of incomplete Freund's adjuvant and C57BL/6J mice were immunized subcutaneously (s.c.) and intraperitoneally (i.p.). 6 weeks after immunization, a 50 µg boost injection was applied i.p. and s.c. three days before isolation and fusion of the splenic B cells with the myeloma cell line P3X63Ag8.653 (performed using polyethylene glycol 1500 according to standard protocols).¹¹ Hybridoma supernatants were tested by solid-phase enzyme-linked immunoassay (ELISA) using GST-COMMD6 fusion protein and verified by Western blot. The hybridoma cells of COMMD6-reactive supernatant 26F7 were cloned twice by limiting dilution. The IgG subclass clone 26F7 was determined with ELISA assay as mouse IgG2a kappa light chain. All experiments targeting mouse COMMD6 were performed with this antibody.

Isotopically labeled standard for targeted proteomics

To quantify the protein concentrations of the COMMDs, components of retromer, the CCC and WASH complexes, LDLR and LRP1 in the liver homogenates and APOA1 and APOB in plasma of the different mouse models we developed targeted proteomics assay. Isotopically labeled peptide standards were used to develop targeted LC-MS assays through selection of optimal MS settings for two peptides per targeted protein. Quantotypic peptides were selected for both mouse and human orthologs, based on selection criteria described previously.¹² All target peptides were concatenated into synthetic proteins (Polyquant GmbH, Germany) containing ¹³C-labeled lysines and arginines (so-called QconCATs). The mouse specific peptide targets for this study are listed in Supplementary Table S2. Additional ¹³C¹⁵N-labeled lysine containing synthetic peptides (AQUA QuantPro, Thermo Scientific) were added for COMMD1 to include peptide variants resulting from missed cleavage (sequence motifs causing incomplete digest of COMMD1), since the initially selected peptide for COMMD1 (without missed cleavages) did not yield a LC-MS response above the detection limit (Supplementary Table S2).

In-gel digestion and sample cleanup for mass spectrometry analysis

For immunoprecipitated (IP) enriched protein samples in SDS loading buffer (0.01% bromophenol blue, 2% SDS, 4% glycerol, 1% β-mercaptoethanol in 150 mM Tris buffer (pH 6.8)), 20 µL total volume was loaded on the gel. For plasma samples 1 µL plasma plus 1 ng QconCATs were loaded on the gel. For liver tissue samples: 40 µg total protein plus 28.7 fmol QconCAT were loaded on the gel and samples were run briefly into a precast 4–12% Bis-Tris gel (Novex, ran for a maximum of 5 min at 100 V). The sample was run briefly into a precast 4–12% Bis-Tris gel (Novex, ran for maximally 5 min at 100V). The gel was stained with Biosafe Coomassie G-250 stain (Biorad) and after destaining with milliQ, one band containing all proteins was excised from the gel.

The gel was stained with Biosafe Coomassie G-250 stain (Bio-Rad). After destaining with milliQ, one band containing all proteins was excised from the gel. To quantify the concentrations of the COMMD proteins in liver lysates the same samples were also loaded into a precast 4–12% Bis-Tris gel (Novex), and were run for approximately 15 min at 100 V. In this way, the small proteins were separated from the larger, more abundant proteins. The gel was stained with Biosafe Coomassie G-250 stain (Bio-Rad) and after destaining with milliQ, gel bands containing proteins (including COMMD proteins) with a molecular weight between 5–25 kDa were excised from the gel.

Each excised gel band was sliced into small pieces, washed subsequently with 30% and 50% v/v acetonitrile with 100 mM ammonium bicarbonate, and incubated at RT for 30 min while mixing (500 rpm). Then, 100% acetonitrile was added for 5 min and the gel pieces were dried at 37°C. The proteins were reduced with 20 µL 10 mM dithiothreitol (30 min, 55 °C) and alkylated with 20 µL 55 mM iodoacetamide (30 min, in the dark at RT). Then, gel pieces were washed for 30 min with 50% acetonitrile containing 100 mM ammonium bicarbonate while mixing (500 rpm) and dried at 37°C before overnight digestion with 20 µL trypsin (1:100 g/g, sequencing grade modified trypsin V5111, Promega) at 37 °C. The next day, the residual liquid was collected and proteins were eluted from the

gel pieces with 20 μ L 75% v/v acetonitrile containing 5% v/v formic acid (incubation 20 min at RT, mixing 500 rpm).

For liver tissue and plasma samples, the elution fraction was combined with the residual liquid and diluted to 1 mL with 0.1% v/v formic acid for cleanup on a C18-SPE column (SPE C18-Aq 50 mg/1ml, Gracepure). This column was conditioned with 2x1 mL acetonitrile containing 0.1% v/v formic acid and re-equilibrated with 2x1 mL 0.1% v/v formic acid before the samples were loaded. Bound peptides were washed with 2x1 mL 0.1% v/v formic acid and eluted with 2x0.4 mL 50% v/v acetonitrile plus 0.1% v/v formic acid. The eluted fractions were dried under vacuum and resuspended in 20 μ L 0.1% v/v formic acid. For immunoprecipitated samples and fractions enriched for the COMMD proteins the additional cleanup step was omitted, samples were dried under vacuum immediately and resuspended in 10 μ L 0.1% v/v formic acid.

Targeted LC-MS analysis

From the IP samples 3 μ L was injected in the LC-MS after addition of 6.5 fmol pre-digested QconCAT and 225 amol COMMD1-peptides. 2 μ g total protein of liver homogenates plus 1.4 fmol QconCAT were injected into the LC-MS. In case the relative small proteins (5–25 kDa) were analyzed, an equivalent of 11 μ g total protein was injected in the LC-MS after addition of 3.8 fmol pre-digested QconCAT and 133 amol COMMD1-peptides. For plasma an equivalent of 25 nL plasma plus 0.5 ng QconCAT was injected.

Targeted LC-MS analyses were performed on a triple quadrupole mass spectrometer with a nano-electrospray ion source (TSQ Vantage, Thermo Scientific). Chromatographic separation of the peptides was performed by liquid chromatography on a nano-UHPLC system (Ultimate 3000, Dionex) using a nano-LC column (Acclaim PepMap100 C18, 75 μ m x 500 mm, 2 or 3 μ m, 100 \AA , Dionex). Samples were injected using the μ L-pickup method with 0.1% v/v formic acid as a transport liquid from a cooled autosampler (5°C) and loaded onto a trap column (μ Precolumn cartridge, Acclaim PepMap100 C18, 5 μ m, 100 \AA , 300 μ m x 5 mm, Dionex). Peptides were separated on the nano-LC column using a linear gradient from 3–60 % v/v acetonitrile plus 0.1% v/v formic acid for 100 min at a flowrate of 200 nL/min. The mass spectrometer was operated in positive mode at a spray voltage of 1500 V, a capillary temperature of 270°C, a half maximum peak width of 0.7 for Q1 and Q3, a collision gas pressure of 1.2 mTorr and a cycle time of 1.2 ms. Optimal collision energies (CE) were predicted using the following linear equations: $CE = 0.03 * m/z \text{ precursor ion} + 2.905$ for doubly charged precursor ions, and $CE = 0.03 * m/z \text{ precursor ion} + 2.467$ for triply charged precursor ions. For each of the peptides, the optimal precursor charge and three optimal transitions were selected after screening with the QconCAT peptides. The measurements were scheduled in windows of 5 min around the pre-determined retention time. The LC-MS peak assignments were manually curated using Skyline software¹³ and the integration peak areas can be used for quantification using the known concentration of the spiked isotopically labelled standard. For qualitative purposes, the targets were considered specifically IP enriched if the isotopically spiked peptides were detected in both IP and control samples, but the endogenous peptide was detected only in the IP sample and not in the control sample. The targets were considered absent (or below the limit of detection) if the endogenous peptides were not detected in both samples, but the isotopically labelled standards were detected in both.

Biotinylation assay

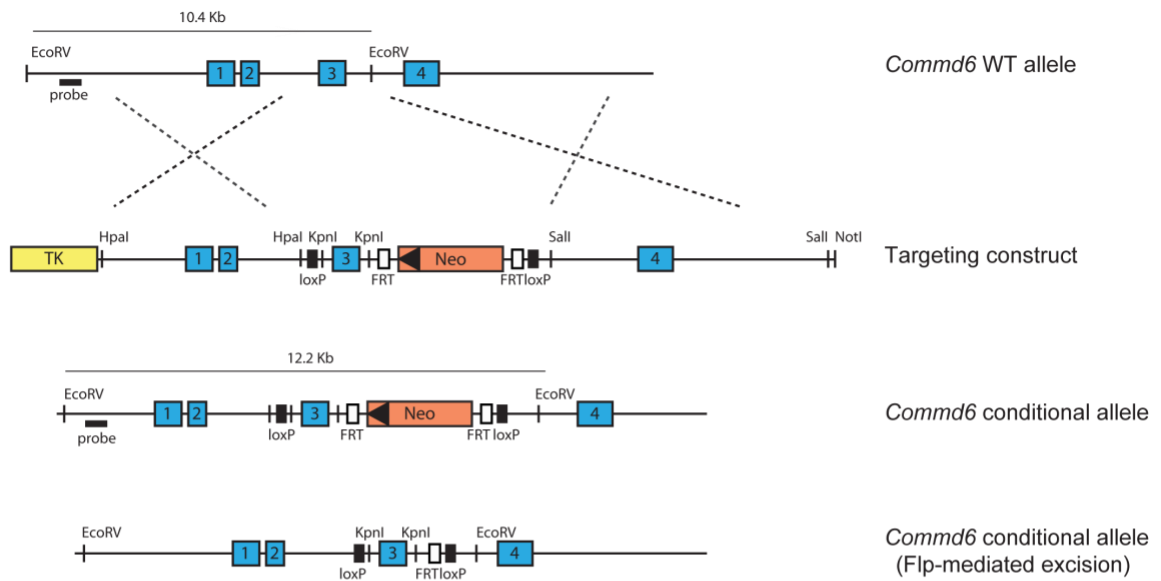
Culture of primary hepatocytes and biotinylation assay were performed as previously described.¹⁴ Cells were washed 3x with ice-cold PBS-CM buffer (PBS, 1mM MgCl₂ and 0.1mM CaCl₂), subsequently 0.5mg/ml biotin reagent solution (EZ-Link Sulfo-NHS-SS_Biotin, Thermo Scientific) in biotinylation buffer (10mM triethanolamine, pH 8.0, 150mM NaCl and 2mM CaCl₂) was added to the cells for 30 min at 4°C. Biotin reagent was removed and cells were washed 1x with quenching buffer (PBS-CM, 25mM Tris-HCl, pH 7.4 and 192mM Glycine) for 30 min at 4°C. Next, cells were washed 2x with PBS-CM and 1x with TBS-C (50mM Tris-Cl, pH 7.4, 100mM NaCl and 2mM CaCl₂). Cells were collected by scraping in TBS-C. Cells were centrifuged (1,000g, 5 min, 4°C), lysed in biotin lysis buffer (50mM Tris-Cl, pH 7.4, 150mM NaCl, 1% NP-40, 0.5% sodium deoxycholate, 5mM EDTA and 5mM EGTA), sonicated (10% output for 10 s) and incubated on ice for 15 min, subsequently centrifuged for 15 min at 12,000 g. Protein concentration was determined; 30 mg was used as input; 300 mg was used diluted in biotin lysis buffer (500 μ l); 30 μ l Neutravidin beads (Neutravidin plus ultralink beads, Thermo

Scientific) was added and incubated for 4 h at 4°C. Beads were collected by centrifugation (500g, 5min), beads were washed 3x with Biotin lysis buffer, 1x with high-salt buffer (50mM Tris-Cl, pH 7.4 and 500mM NaCl) and 1x with low-salt buffer (10mM Tris-HCl). Finally, the beads were resuspended in 30µl 2x loading buffer.

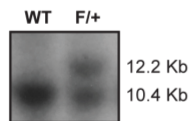
References

1. Dawlaty MM, van Deursen JM. Gene targeting methods for studying nuclear transport factors in mice. *Methods*. 2006;39:370-378.
2. Vonk WI, Bartuzi P, de Bie P, Kloosterhuis N, Wichers CG, Berger R, Haywood S, Klomp LW, Wijmenga C, van de Sluis B. Liver-specific CommD1 knockout mice are susceptible to hepatic copper accumulation. *PLoS One*. 2011;6:e29183.
3. Li H, Koo Y, Mao X, Sifuentes-Dominguez L, Morris LL, Jia D, Miyata N, Faulkner RA, van Deursen JM, Vooijs M, Billadeau DD, van de Sluis B, Cleaver O, Burstein E. Endosomal sorting of notch receptors through COMMD9-dependent pathways modulates notch signaling. *J Cell Biol*. 2015;211:605-617.
4. Platt RJ, Chen S, Zhou Y, Yim MJ, Swiech L, Kempton HR, Dahlman JE, Parnas O, Eisenhaure TM, Jovanovic M, Graham DB, Jhunjhunwala S, Heidenreich M, Xavier RJ, Langer R, Anderson DG, Hacohen N, Regev A, Feng G, Sharp PA, Zhang F. CRISPR-Cas9 knockin mice for genome editing and cancer modeling. *Cell*. 2014;159:440-455.
5. Bjorklund MM, Hollensen AK, Hagensen MK, Dagnaes-Hansen F, Christoffersen C, Mikkelsen JG, Bentzon JF. Induction of atherosclerosis in mice and hamsters without germline genetic engineering. *Circ Res*. 2014;114:1684-1689.
6. Levels JH, Lemaire LC, van den Ende AE, van Deventer SJ, van Lanschot JJ. Lipid composition and lipopolysaccharide binding capacity of lipoproteins in plasma and lymph of patients with systemic inflammatory response syndrome and multiple organ failure. *Crit Care Med*. 2003;31:1647-1653.
7. van de Sluis B, Muller P, Duran K, Chen A, Groot AJ, Klomp LW, Liu PP, Wijmenga C. Increased activity of hypoxia-inducible factor 1 is associated with early embryonic lethality in CommD1 null mice. *Mol Cell Biol*. 2007;27:4142-4156.
8. de Bie P, van de Sluis B, Burstein E, Duran KJ, Berger R, Duckett CS, Wijmenga C, Klomp LW. Characterization of COMMD protein-protein interactions in NF-kappaB signalling. *Biochem J*. 2006;398:63-71.
9. Ran FA, Hsu PD, Wright J, Agarwala V, Scott DA, Zhang F. Genome engineering using the CRISPR-Cas9 system. *Nat Protoc*. 2013;8:2281-2308.
10. Gomez TS, Billadeau DD. A FAM21-containing WASH complex regulates retromer-dependent sorting. *Dev Cell*. 2009;17:699-711.
11. Kohler G, Milstein C. Continuous cultures of fused cells secreting antibody of predefined specificity. *Nature*. 1975;256:495-497.
12. van Eunen K, Volker-Touw CM, Gerding A, Bleeker A, Wolters JC, van Rijt WJ, Martines AM, Niezen-Koning KE, Heiner RM, Permentier H, Groen AK, Reijngoud DJ, Derks TG, Bakker BM. Living on the edge: Substrate competition explains loss of robustness in mitochondrial fatty-acid oxidation disorders. *BMC Biol*. 2016;14:107.
13. MacLean B, Tomazela DM, Shulman N, Chambers M, Finney GL, Frewen B, Kern R, Tabb DL, Liebler DC, MacCoss MJ. Skyline: An open source document editor for creating and analyzing targeted proteomics experiments. *Bioinformatics*. 2010;26:966-968.
14. Lagace TA, Curtis DE, Garuti R, McNutt MC, Park SW, Prather HB, Anderson NN, Ho YK, Hammer RE, Horton JD. Secreted PCSK9 decreases the number of LDL receptors in hepatocytes and in livers of parabiotic mice. *J Clin Invest*. 2006;116:2995-3005.

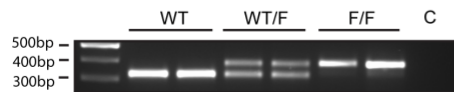
A.



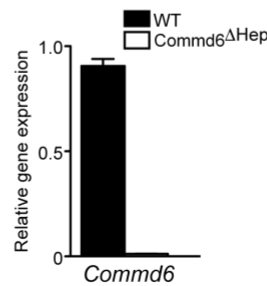
B.



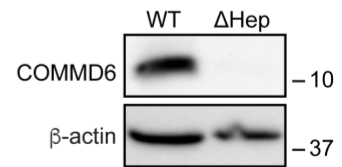
C.



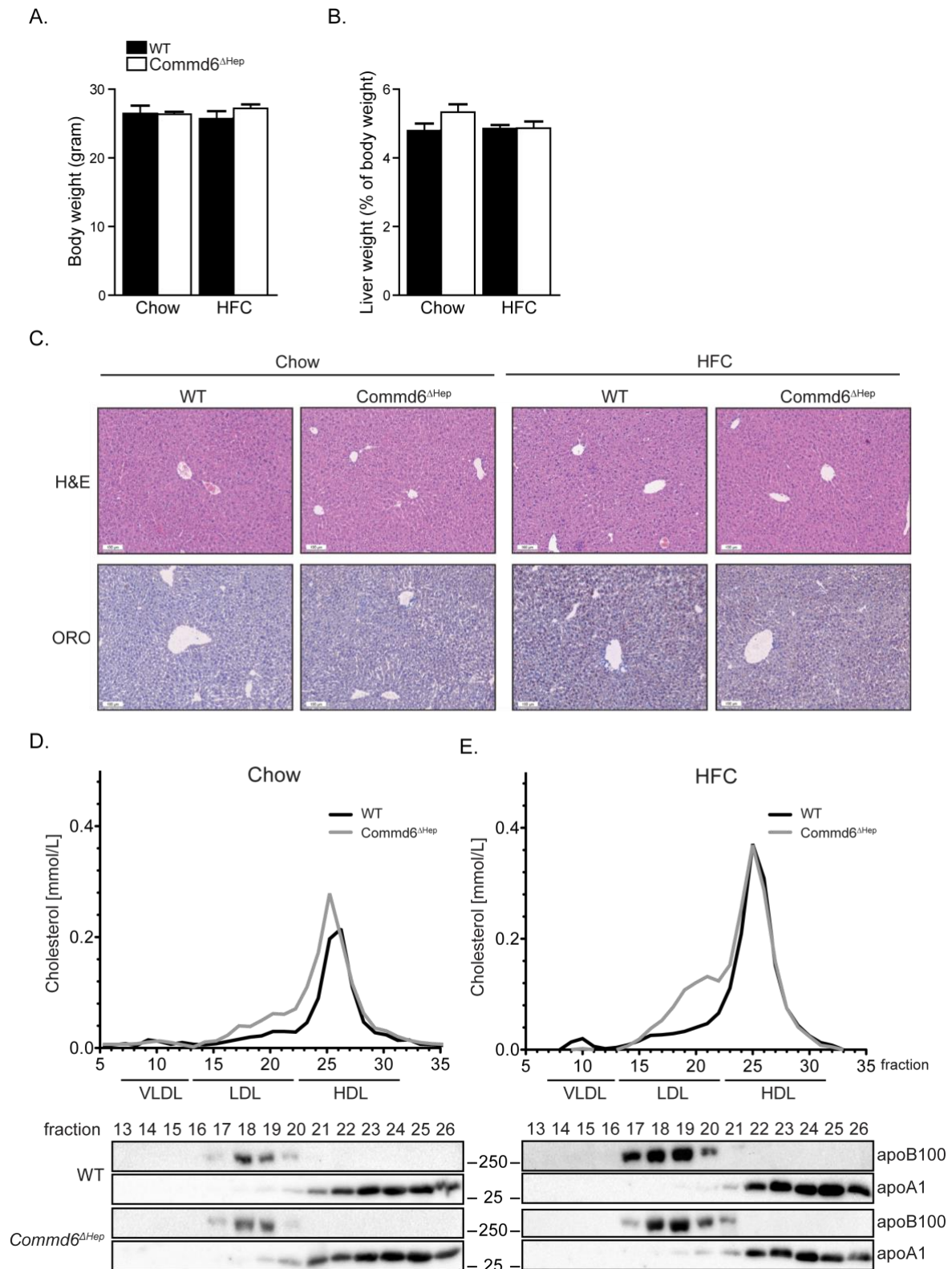
D.



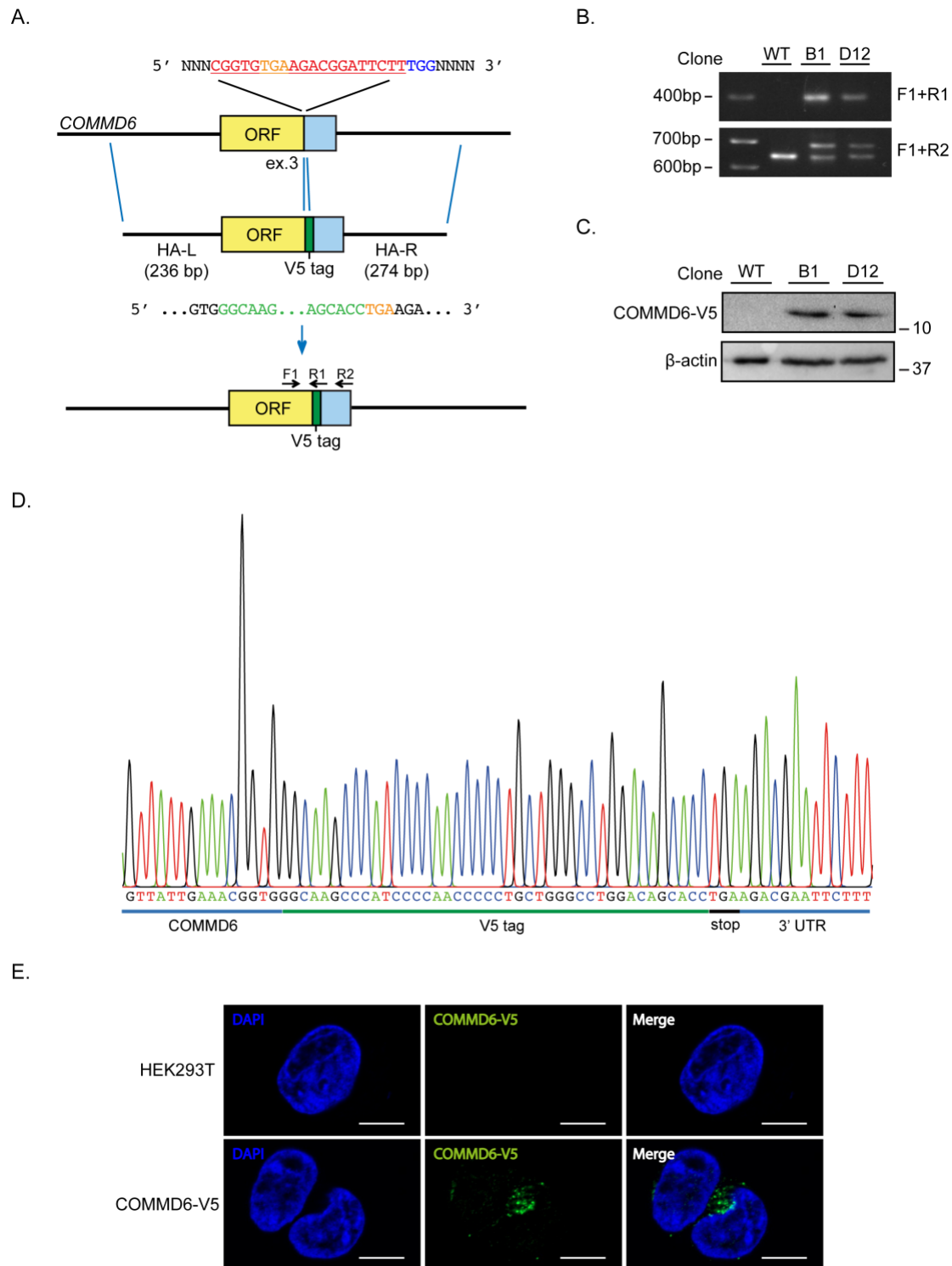
E.



Online Figure I. Generation of hepatocyte-specific *Commd6* knockout mice. (A) Schematic representation of the *Commd6* gene targeting strategy to generate a conditional *Commd6* knockout allele. A genetic map of *Commd6*, the targeting vector, the *Commd6* locus after homologous recombination, and the final conditional *Commd6* knockout allele after Flp-mediated excision of the Neo cassette are illustrated. Depicted are the *Commd6* exons (blue boxes), loxP sites (black boxes), FRT sites (white boxes) and neomycin selection gene (Neo). Homologous recombination is marked with dotted lines. (B) Southern blot of *EcoRV* digested genomic DNA from two ES cell clones and probed for the DNA fragment indicated in (A). The 10.4 kb and 12.2 kb fragments represent the wild type (WT) and *Commd6* floxed allele, respectively. (C) PCR genotyping of two WT, WT/loxP and loxP/loxP mice without the Neo cassette. C represents a negative control (H₂O). (D) *Commd6* mRNA expression in livers of *Commd6*^{ΔHep} and WT mice (n=7–9). (E) Immunoblot analysis showing COMMD6 protein levels in the liver of WT and *Commd6*^{ΔHep} mice. Group averages and SEM are shown.

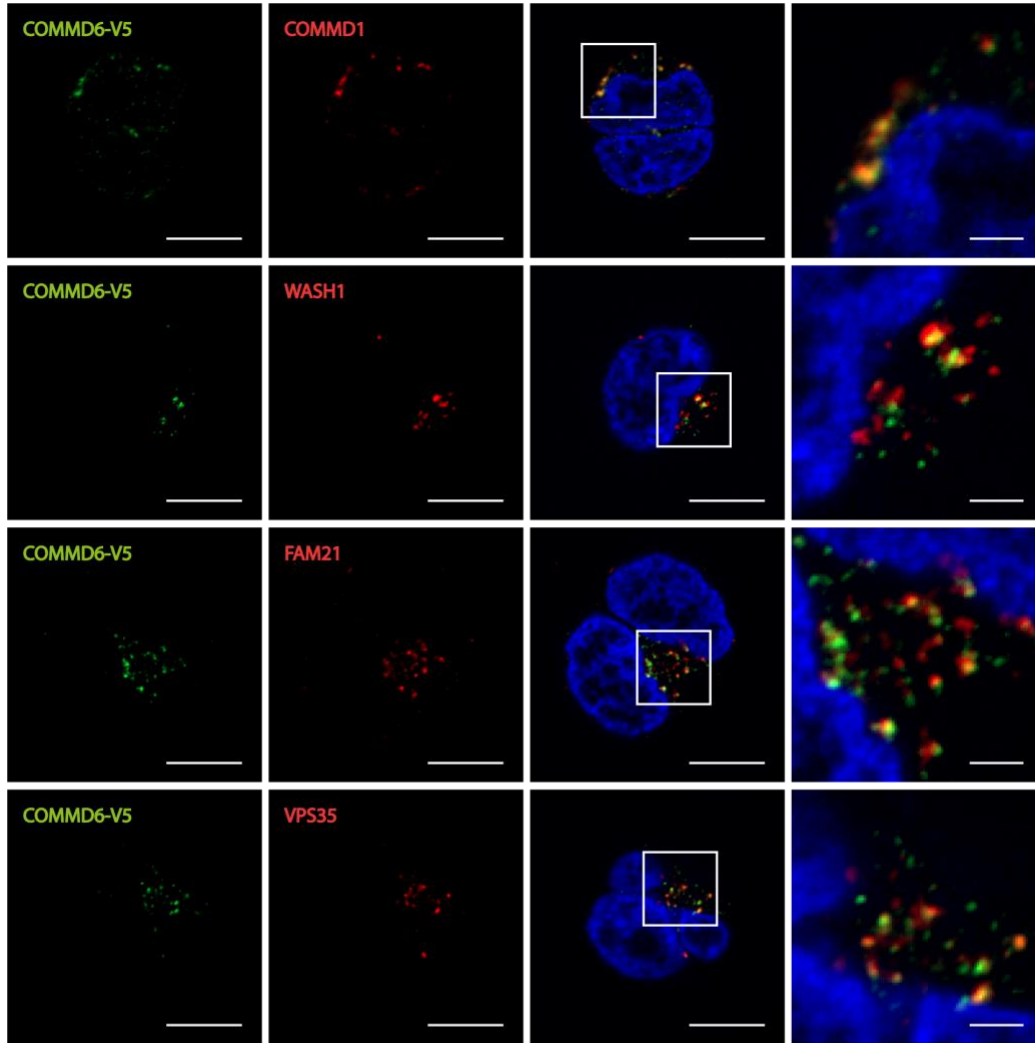


Online Figure II. Body weight, liver weight and liver histology are unaffected by hepatic COMMD6 deficiency. Body weight (**A**) and liver weight as percentage of body weight (**B**) for WT and *Commd6*^{ΔHep} mice (n=7–9). (**C**) H&E and ORO staining of hepatic tissue from WT and *Commd6*^{ΔHep} mice fed a chow or a HFC diet for 1 week. Representative images shown, scale bar = 100 μm. Total cholesterol levels of FPLC fractionated pooled plasma sample of the experimental groups of mice fed either a chow (**D**) or a HFC (**E**) diet (n=7–9). Immunoblotting of ApoB100 and ApoA1 was performed on fractions #13–26. Group averages and SEM are shown.

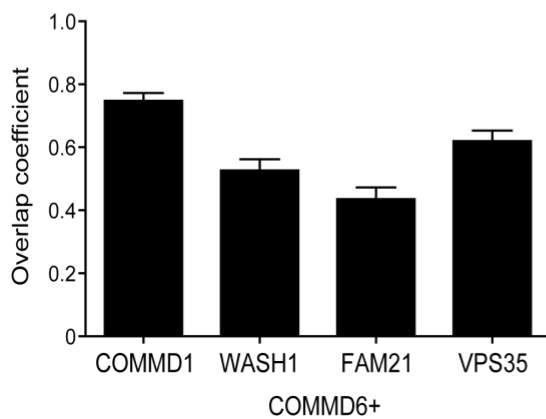


Online Figure III. Generation of a V5 tagged *COMMD6* allele in HEK293T cells. (A) Schematic representation of the construct used to edit endogenous *COMMD6*. Annotated are the gRNA target sequence (red), stop codon (orange) and PAM sequence (blue). The repair construct consisted of a V5 tag (green), which was introduced right before the stop codon (orange) of *COMMD6*, and two homology arms (HA-L and HA-R) for homologous recombination (blue lines). F1, R1 and R2 represent the primers used to confirm V5 insertion via PCR. **(B)** PCR analysis of wild type and V5-tagged HEK293T monoclonal cell lines (B1 and D12). **(C)** Western blotting of V5 and β -actin in wild type and COMMD6-V5 HEK293T cell lysates. **(D)** Sequence throughout the V5-targeted region to confirm correct fusion of the V5-tag to the last codon of *COMMD6*. **(E)** Immunofluorescence staining of COMMD6-V5 in HEK293T wild type and COMMD6-V5 monoclonal cell lines (B1).

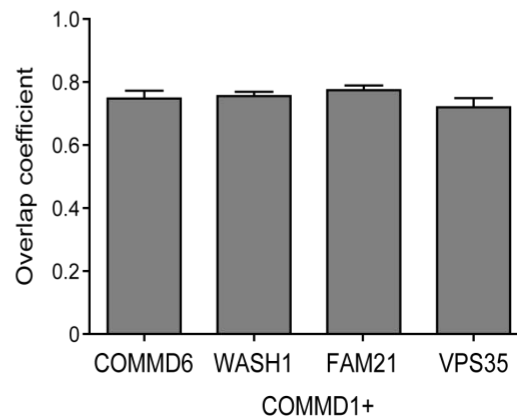
A.



B.

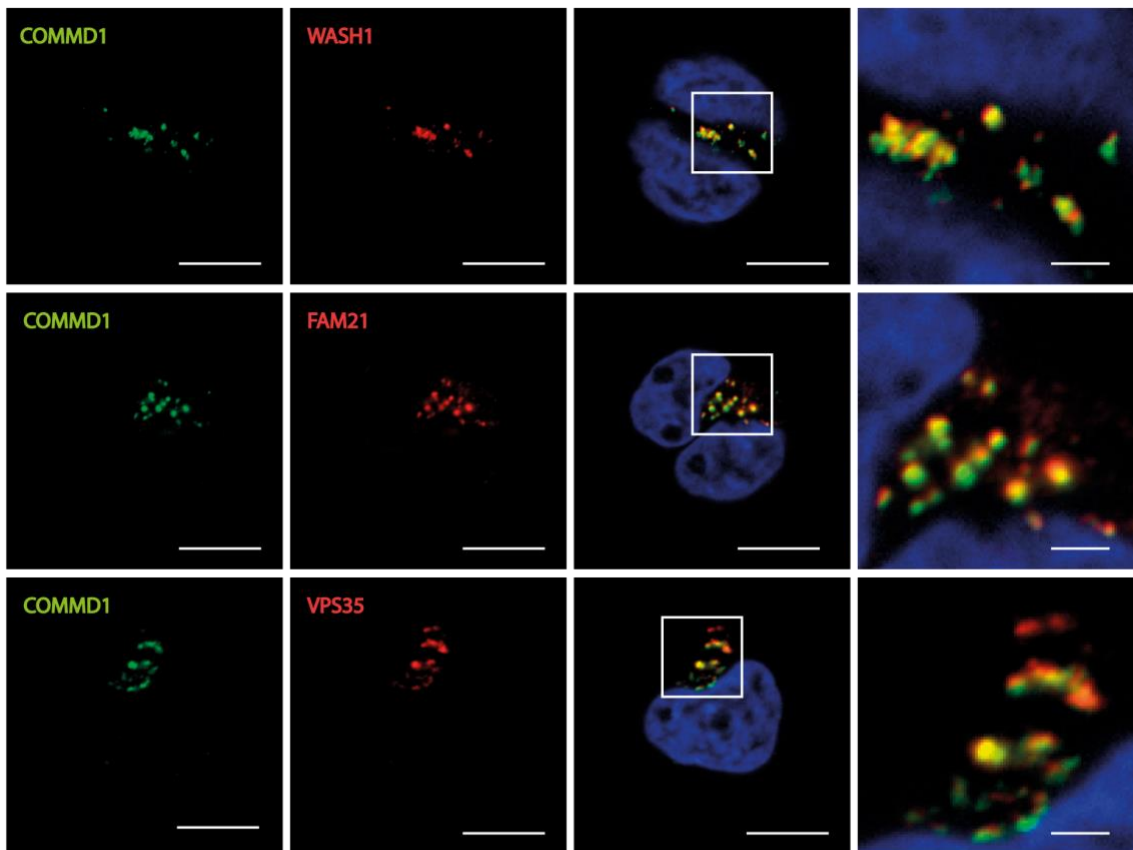


C.

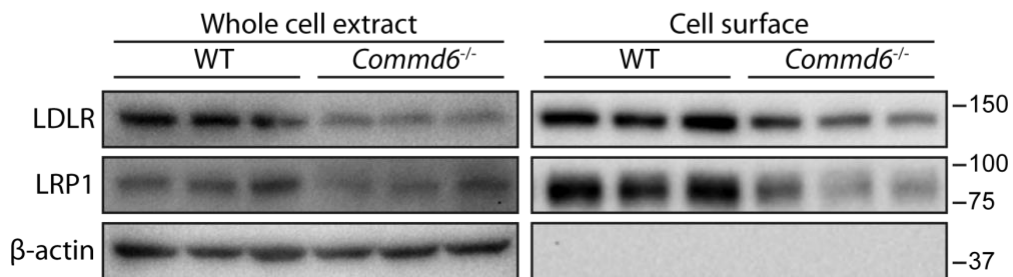


Online Figure IV. Subcellular localization of COMMD6 overlaps with COMMD1, WASH complex and retromer. (A) Cellular localization of COMMD6-V5 (green), COMMD1 (red), WASH1 (red), FAM21 (red) and VPS35 (red) in HEK293T cells expressing endogenous V5-tagged COMMD6 determined by indirect immunofluorescence staining. DAPI (blue) was used to stain nuclear DNA. Representative images are shown. Scale bar = 10 μ m. Overlap coefficient of COMMD6 (B) and COMMD1 (C) with each other, the WASH complex subunits WASH1 and FAM21, and retromer component VPS35. Group averages and SEM are shown ($n \geq 30$).

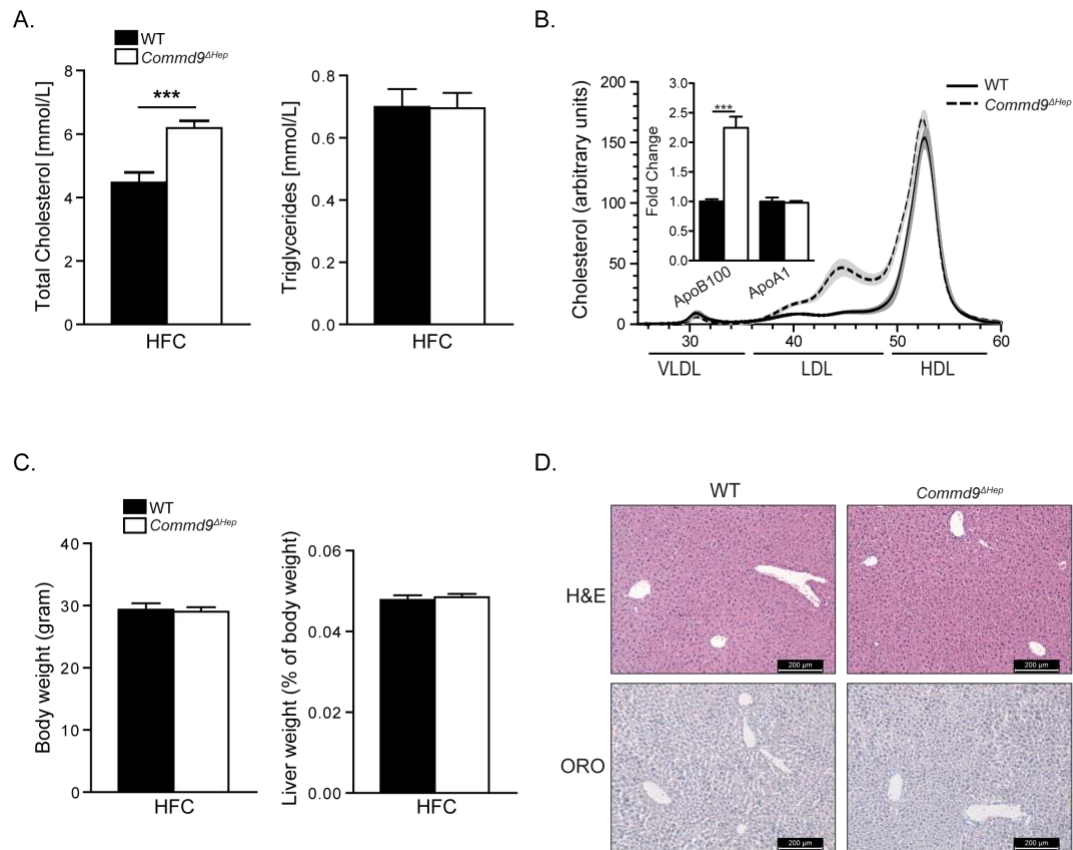
A.



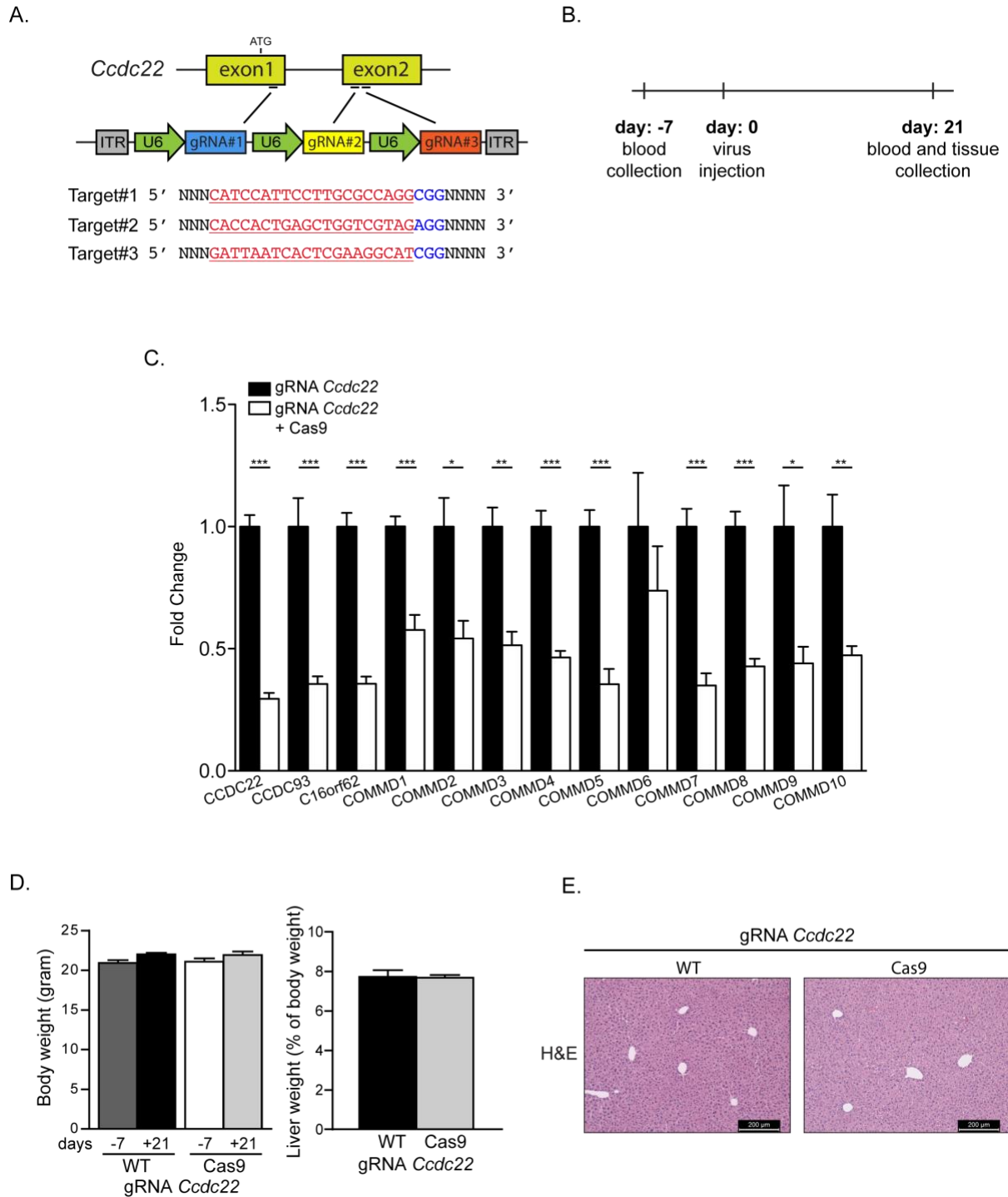
B.



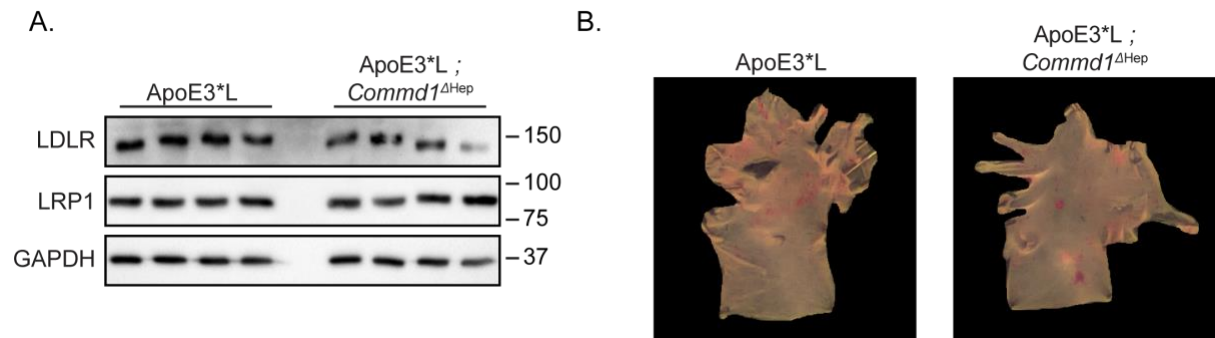
Online Figure V. Subcellular localization of COMMD1 overlaps with the WASH complex and retromer. (A) Cellular localization of COMMD1 (green), WASH1 (red), FAM21 (red) and VPS35 (red) in the HEK293T COMMD6-V5 monoclonal cell line, determined by immunofluorescence staining. Representative images shown, scale bar = 10 μm. (B) Whole cell and cell surface levels of LDLR and LRP1 in WT and *Commd6*^{-/-} primary hepatocytes.



Online Figure VI. Hepatic COMMD9 regulates plasma cholesterol. (A) Plasma cholesterol and triglyceride levels of WT and *Commd9^{ΔHep}* animals after one week of HFC feeding (n=6). (B) Total cholesterol levels of pooled FPLC fractionated plasma samples of mice fed a HFC diet for one week (n=6). (Inset B) Plasma ApoB100 and ApoA1 levels of *Commd9^{ΔHep}* and WT, indicated by fold change versus WT controls (n=6) (C) Body weight and liver weight as a percentage of body weight of WT and *Commd9^{ΔHep}* animals after one week of HFC feeding (n=6). (D) H&E and ORO staining of hepatic tissue from WT and *Commd9^{ΔHep}* mice after one week of HFC feeding. Representative images shown, scale bar = 200 μm. Group averages and SEM are shown. ***p<0.001 (compared to controls).

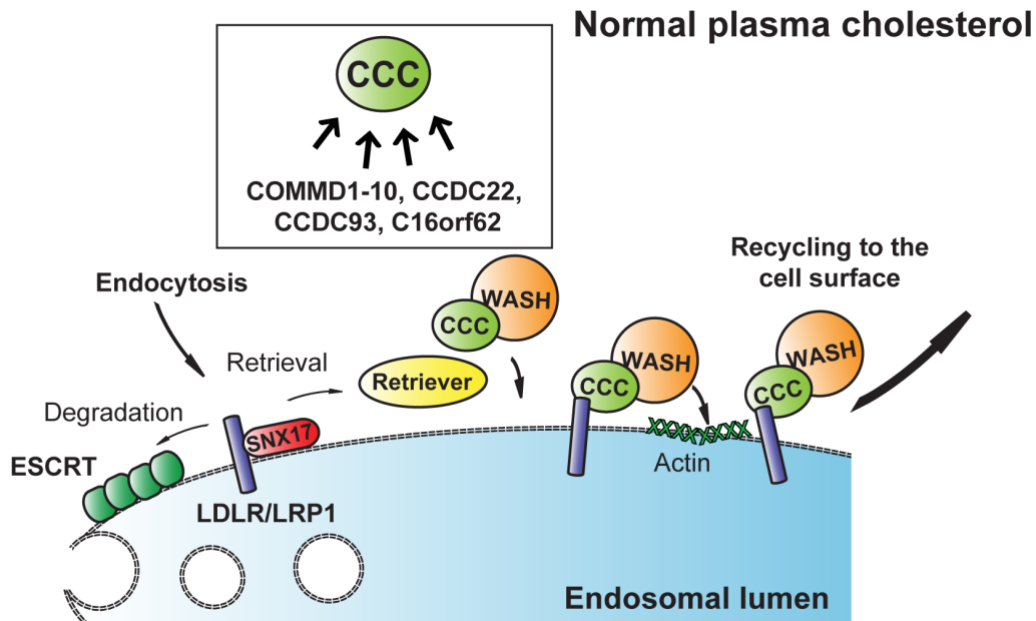


Online Figure VII. Body weight, liver weight and liver histology are not affected by hepatic CCDC22 insufficiency. (A) Schematic representation of the single-vector AV system to target *Ccdc22* in parenchymal cells of hepatic Cas9-expressing mice. Annotated are the target sequences (red) and PAM sequences (blue) of the gRNAs. (B) Experimental timeline of the CRISPR/Cas9-mediated gene editing approach. (C) Fold change of protein levels of CCC core complex components and COMMD proteins after CRISPR/Cas9-mediated *Ccdc22* editing (n=4) (D) Body weight and liver weight as a percentage of body weight of WT and Cas9 animals injected with AV-gRNA-*Ccdc22* (n=5-6). (E) H&E staining of hepatic tissue of WT and Cas9 animals injected with AV-gRNA-*Ccdc22*. Representative images shown, scale bar = 200 μm.

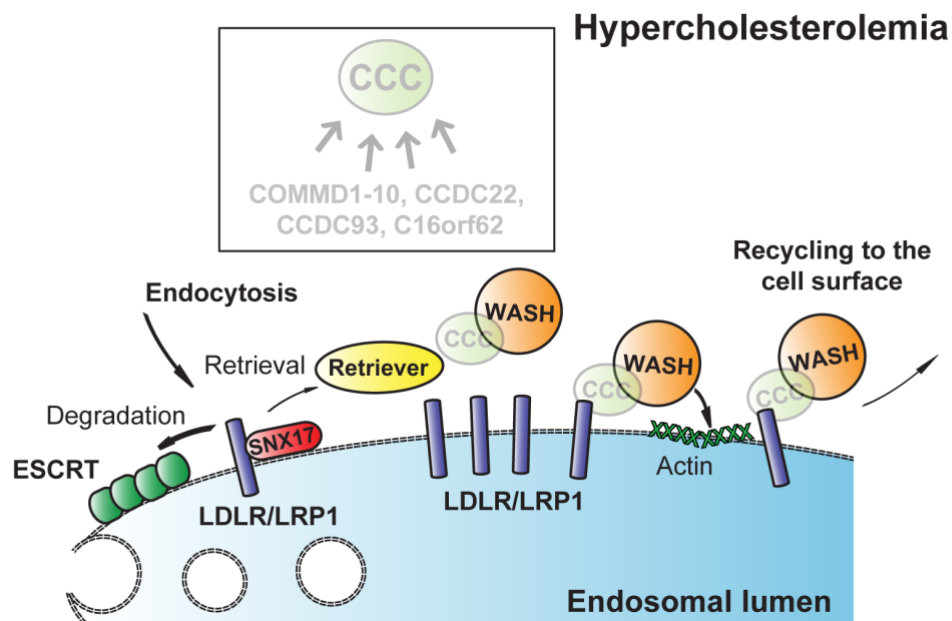


Online Figure VIII. Lipid-rich plaques in the aortic arch of ApoE3*L and ApoE3*L;*Commd1*^{ΔHep} animals. (A) Total liver protein levels of LDLR and LRP1 in ApoE3*L and ApoE3*L;*Commd1*^{ΔHep} animals, as determined by immunoblotting. (B) Representative images of Oil Red-O stained aortic arch of ApoE3*L and ApoE3*L;*Commd1*^{ΔHep} animals.

A.



B.



Online Figure IX. Hypothetical model of the CCC-WASH axis in endosomal LDLR and LRP1 trafficking. (A) On entering the endosomal network LDLR and LRP1 are subjected to one of two fates decisions, either the receptors are sorted into the lysosome for proteolysis, likely through the endosomal sorting complexes required for transport (ESCRT), or the receptors are retrieved and are recycled back to cell surface to take up the next cargo. We speculate that SNX17 is a LDLR and LRP1-specific adaptor allowing the receptors to enter into retrieval and recycling pathway, which is coordinated by the retriever (DSCR3, C16orf62, VPS29), the CCC complex and WASH complex. The recruitment of the CCC and WASH complexes to the endosomes may be dependent on the retromer subunit VPS35. (B) Depletion of one component (either a COMMD protein or a CCC core component) of the CCC complex destabilizes the complete CCC complex leading to impaired endosomal trafficking of LDLR and LRP1 resulting in enhanced ESCRT-mediated sorting into the lysosomes, decreased surface levels of LDLR and LRP1 and consequently hypercholesterolemia and enhanced atherogenesis.

Online Table I. Relative protein levels of the proteins studied.

Relative protein abundance (relative to WT samples)	C1 KO (n=4)	C6 KO (n=4)	C9 KO (n=4)	C1 WT (n=4)	C6 WT (n=4)	C9 WT (n=4)	C1 KO SEM	C6 KO SEM	C9 KO SEM	C1 WT SEM	C6 WT SEM	C9 WT SEM	P-value C1 KO vs WT	P-value C6 KO vs WT	P-value C9 KO vs WT
COMMD1	0,24	0,26	0,56	1,00	1,00	1,00	0,04	0,04	0,11	0,08	0,13	0,05	6E-05	9E-04	4E-03
COMMD2	0,50	0,52	0,48	1,00	1,00	1,00	0,05	0,04	0,07	0,05	0,11	0,05	3E-04	3E-03	4E-04
COMMD3	0,53	0,45	0,56	1,00	1,00	1,00	0,04	0,03	0,05	0,15	0,18	0,08	7E-04	2E-02	1E-03
COMMD4	0,29	0,27	0,38	1,00	1,00	1,00	0,05	0,05	0,05	0,16	0,28	0,08	3E-03	2E-02	3E-04
COMMD5	0,22	0,25	0,21	1,00	1,00	1,00	0,03	0,01	0,02	0,12	0,23	0,06	4E-04	9E-03	7E-06
COMMD6	0,36	0,32	0,68	1,00	1,00	1,00	0,07	0,06	0,14	0,26	0,27	0,10	3E-02	3E-02	5E-02
COMMD7	0,35	0,24	0,23	1,00	1,00	1,00	0,04	0,02	0,01	0,07	0,26	0,06	1E-04	1E-02	6E-06
COMMD8	0,36	0,26	0,63	1,00	1,00	1,00	0,05	0,03	0,10	0,11	0,20	0,08	9E-04	5E-03	1E-02
COMMD9	0,41	0,31	0,23	1,00	1,00	1,00	0,06	0,03	0,02	0,07	0,14	0,02	3E-04	2E-03	2E-07
COMMD10	0,32	0,28	0,39	1,00	1,00	1,00	0,02	0,03	0,05	0,14	0,29	0,06	1E-03	2E-02	9E-05
CCDC22	0,33	0,25	0,33	1,00	1,00	1,00	0,02	0,02	0,04	0,07	0,11	0,08	5E-05	3E-04	7E-05
CCDC93	0,33	0,22	0,33	1,00	1,00	1,00	0,02	0,07	0,05	0,08	0,16	0,05	1E-04	2E-03	2E-05
C16orf62	0,28	0,24	0,36	1,00	1,00	1,00	0,01	0,05	0,07	0,06	0,15	0,05	1E-05	1E-03	2E-05
LDLR	1,24	1,17	1,13	1,00	1,00	1,00	0,08	0,11	0,07	0,08	0,07	0,13	6E-02	6E-02	2E-01
LRP1	1,00	0,77	1,08	1,00	1,00	1,00	0,03	0,19	0,07	0,07	0,15	0,08	5E-01	9E-02	3E-01
WASH1	1,58	1,71	1,06	1,00	1,00	1,00	0,14	0,16	0,09	0,11	0,18	0,06	4E-03	4E-03	3E-01
CCDC53	1,28	0,99	1,62	1,00	1,00	1,00	0,21	0,11	0,21	0,11	0,17	0,10	1E-01	5E-01	8E-03
Strumpellin	1,16	1,11	1,14	1,00	1,00	1,00	0,07	0,07	0,12	0,06	0,13	0,04	1E-01	2E-01	7E-02
VPS35	1,05	0,91	1,23	1,00	1,00	1,00	0,05	0,14	0,16	0,08	0,15	0,06	4E-01	3E-01	7E-02
VPS26A	1,00	0,99	0,80	1,00	1,00	1,00	0,07	0,12	0,17	0,07	0,17	0,05	5E-01	5E-01	6E-02
VPS29	0,80	0,84	0,75	1,00	1,00	1,00	0,07	0,06	0,07	0,08	0,18	0,06	4E-02	2E-01	2E-02

Online Table II. List of peptides used for targeted proteomics.

Protein target	Peptide	Comments
C16orf62	FVLITDILDTFGK	
C16orf62	GIGDPLVSVYAR	
CCDC22	DLLLFLAER	
CCDC22	TFAVTDELVFK	
CCDC53	IQQIETTLNILDAK	
CCDC53	LADLSLR	
CCDC93	GPEGQGLPEVETR	
CCDC93	IALSEK	
COMMD1*	HSTQIHSPVAHIELEFGK	low response in the MS
COMMD1*	KQGGITSEQAAVISK	synthetic peptide, endogenous concentration calculated by sum of endogenous QGGITSEQAAVISK + KQGGITSEQAAVISK
COMMD1*	QGGITSEQAAVISK	synthetic peptide, endogenous concentration calculated by sum of endogenous QGGITSEQAAVISK + KQGGITSEQAAVISK
COMMD10*	ELDFDFYNK	
COMMD10*	LQAAFSLEK	
COMMD2*	LDVQLASR	
COMMD2*	QQIKPAVTIK	
COMMD3*	LEYQIK	
COMMD3*	SLPHITDVSWR	
COMMD4*	FESGDVK	
COMMD4*	FQVLLAELK	
COMMD5*	SLQPSVLMQLK	risk methionine-oxidation, preferably use other peptide for quantification
COMMD5*	YSVALVLK	
COMMD6*	YPYVAVMLK	risk methionine-oxidation, preferably use other peptide for quantification
COMMD6*	SEVTGQLIDFQWK	
COMMD7*	FGVTSGSSELEK	
COMMD7*	VGSIFLQLK	
COMMD8*	LALSSDK	

Online Table II continue

COMMD8*	HVLEDVTTFFK	
COMMD9*	DLSSAEAILALFPENFHQNLK	
COMMD9*	LVDL DWR	
FAM21	DLYIDRPLPYLIGSK	
FAM21	STGVFQDEELLSHK	
KIAA1033 (SWIP)	NSAEGTEYFK	
KIAA1033 (SWIP)	NSTFAEEFAHSIR	
LDLR	NVVALDTEVTNNR	
LDLR	SQDGYTYPSR	
LRP1	AVTDEEPFLIFANR	
LRP1	TTLLAGDIEHPR	
Strumpellin (SPG8)	LASALDLPLLR	
Strumpellin (SPG8)	YIVDLNR	
VPS26A	ELALPGELTQSR	
VPS26A	HYLFYDGESVSGK	
VPS29*	TLAGDVHIVR	
VPS29*	VVTVGQFK	
VPS35	AELAELPLR	
VPS35	ILVGTNLVR	
WASH1	EVVDPSSGR	
WASH1	GPSTGTSEGPGGAFSR	
APOA1	DFWDNLEK	
APOB	QSFDSL VK	peptide detecting APOB100 only#
APOB	VQGV EFSHR	peptide detecting the sum of APOB100+APOB48#

* proteins that were targeted in total liver lysate via excision of the small protein band

The APOB48 concentration was calculated via the difference between the two APOB peptides